Journal of
Mechanical
Science and
Technology

Journal of Mechanical Science and Technology 21 (2007) 1671~1676

A study on the impact behavior of adhesively-bonded composite materials

J. U. Cho[1,*], S. K. Lee[2], C. Cho[2], F. S. Rodriguez Sanchez[3], B. R. K. Blackman[3], A. J. Kinloch[3]

[1]*Department of Mechanical and Automotive Engineering, Kongju University, Boo-dae Dong 275, Cheonan, Korea*

[2]*Department of Mechanical Engineering, Inha University, Yong-hyun Dong 253, Incheon, Korea*

[3]*Department of Mechanical Engineering, Imperial College London, Exhibition Road, London SW7 2AZ, UK*

(Manuscript Received May 31, 2007; Revised August 30, 2007; Accepted September 30, 2007)

Abstract

In this paper, a unidirectional carbon-fiber composite is both experimentally and numerically investigated to study the nonlinear material behavior of impacted double cantilever beam (DCB) specimens. For the impact analysis, the load and the displacement applied from pin onto end block as well as the crack energy release rate are measured and compared with the finite element analysis results. The energy release rate is a critical measure of the resistance to crack propagation, which can be estimated by the force and displacement at the crack tip. It is found that the energy release rate measured from impact tests on the specimens is well predicted by the finite element model suggested in this study.

Keywords: Dynamically loaded; Adhesively bonded specimens; Double cantilever beam specimen; Crack speed; Crack propagation; Energy release rate; Equivalent plastic strain

1. Introduction

The double cantilever beam (DCB) specimen is one of the most commonly used test configurations to measure the fracture toughness of composites and adhesive joints. The application of lightweight high-performance materials like composites and aluminum alloys joined via adhesive bonding is a key enabling technology that can contribute to the development of vehicles with better fuel economy and less emissions, without compromising its performance, comfort, safety and durability. The finite element method was used to analyze the high speed fracture of adhesively bonded composite joints [1, 2]. The toughness of bonded adhesive joints depends on impact rate. High impact rates reduce fracture toughness [3]. Since the composite materials exhibit both plastic and viscoelastic behavior, their deformation depends on the impact speed and temperature [4, 5]. To predict the impact strength it is necessary to calculate the decrease of energy release rate (or fracture energy, G_c) when the adhesively bonded joints are subjected to impact loads. This simulation study investigates and compares the fracture behavior of bonded joints under rapid impacts with experimental results, at various impact rates. The experimental results are taken from [6-8]. In the experiment, the impact rates of 6.4 m/s and 16.7 m/s were applied to the test specimens by the high speed hydraulic test equipment. As the fracture occurred through the adhesively bonded joints, the crack grew rapidly. The crack length and beam displacement were recorded by a high speed camera. This method is used as the impact wedge test by the international standard (ISO 11343) [9]. The crack grows when the applied fracture energy exceeds the value of critical energy release rate (G_{Ic}) at the crack tip. The energy release rate was calculated by classical fracture mechanics formula. The simulation model uses the information of the calculated fracture energy. The configuration of the simulation model is exactly the same as the experiment. The fracture

*Corresponding author. Tel.: +82 41 550 0278, Fax.: +82 41 555 9123
E-mail address: jucho@kongju.ac.kr

behavior is analyzed by a two dimensional finite element method. This model is run by ABAQUS 6.6 [10].

2. Experiment

2.1 Material

A unidirectional carbon-fiber reinforced epoxy-resin composite as 6376/HTA was used in this study. It was a continuous carbon-fiber composite containing the fiber volume fraction of about 63%. This composite is a highly anisotropic, elastic-plastic hardening material with Young's moduli E_{11}=138 GPa, E_{22}=9.9 GPa, G_{12}=12.6 GPa, Poisson's ratio υ=0.22, and density ρ= 1310 kg/m^3. The yield stress and plastic strain values with work hardening are also shown in Table 1.

The fiber composite specimens were prepared in the form of DCB specimens as shown in Fig. 1. The configuration and dimension of specimen are also shown in Fig. 1. The initial cracks in the composite were introduced by inserting an aluminum foil between the substrates. So, the initial delamination is created by molding with a double layer of aluminum foil having the total thickness of 20 μm and the length of 60 mm [11]. The specimen contained a 0.4 mm thick adhesive layer of the XD4600 adhesive from Dow automotive.

2.2 Testing method

The adhesive fracture energy, G_{Ic}, for the adhesive joint specimen in dynamic DCB tests [12] may be determined directly using the Irwin -Kies Eq. (1):

$$G_{IC} = \frac{p^2}{2b}\frac{dC}{da} \tag{1}$$

where p is the applied load, b the specimen width, C the compliance of the substrate beam (given by the displacement divided by the load) and a is the crack length. The value of dC / da is measured experimentally and thus G_{Ic} value can be calculated. The simple beam theory considers the deflections of the beam root rotation which affects both the compliance of the beam and the resulting values of G_{Ic}. Williams [13] showed that the effects of both shear deflection and root rotation could be modeled for a DCB specimen by adding a length, $\triangle$ to the measured crack length as

$$C = \frac{8\left(a+|\Delta|\right)^3}{E_s B h^3} N \tag{2}$$

where h, B and Es are the height, width and Young's modulus of the substrate, respectively. The correction Δ may be found from the negative intercept of a plot of $C^{1/3}$ versus a. When the DCB is held by bonding between the end-blocks, then a correction factor, N in Eq. (2) is employed to correct stiffness due to the presence of the end-blocks and the rotation of the block. Note that N=1 in Eq. (2) when the load is applied to the DCB specimen via holes drilled directly through the substrates. Differentiating Eq. (2),

Table 1. Yield stress and plastic strain with work hardening.

Yield Stress (MPa)	Plastic Strain (%)
700	0
1,000	0.1
1,706	0.107

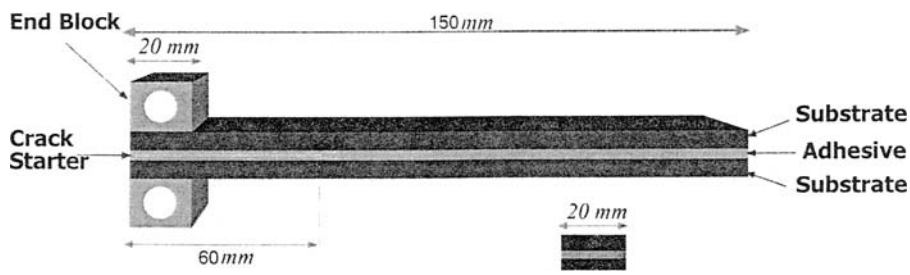

Fig. 1. The configuration and dimension of DCB specimen.

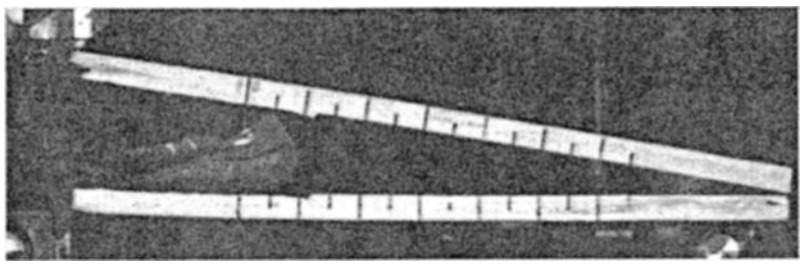

Fig. 2. The picture showing final fractured specimen with the rate of 6.4 m/s.

Fig. 3. The finite element model of the specimen.

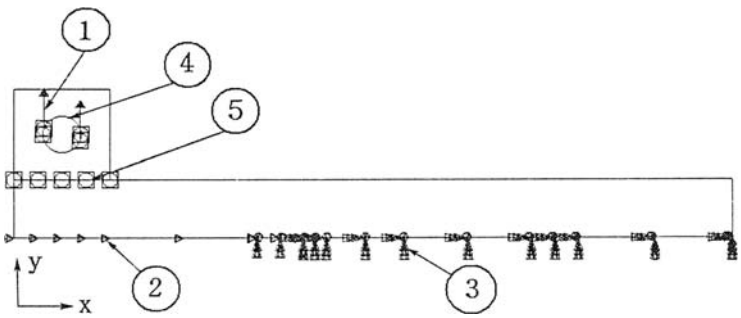

① Round pin applied with the constant velocity of 6.4 m/s or 16.7 m/s
② Fixed displacement of x direction (crack length)
③ Fixed displacements of x and y directions (the rest except crack length)
④ Hard contact between block and pin
⑤ Tied contact between block and specimen

Fig. 4. The boundary conditions at the pin, end block and specimen.

eliminating Es and substituting into Eq. (1) leads to

$$G_{Ic} = \frac{3P\delta}{2B(a+|\Delta|)}\frac{F}{N} \tag{3}$$

where δ is the measured load-line displacement and F is a factor which accounts for the reduction in bending moment caused by large displacements [14]. The picture of a fractured specimen with the rate of 6.4 m/s, for this study, is shown as Fig. 2.

3. Simulation

3.1 Finite element model

Finite element model was developed with ABAQUS code [10]. The geometry and the dimension of the finite element model were the same as those of the specimen shown in Fig. 1. Due to the symmetry, only half a specimen was modeled, and its finite element model is shown in Fig. 3. The 4-node bilinear plane stress quadrilateral elements (CPS4R) are used in the entire FE model. This simulation analysis is undertaken using the explicit method. In this study, the respective number of elements and nodes are 9373 and 9828.

The boundary conditions at the pin, the end block and the specimen are shown in Fig. 4. At the pin, shown by symbol ①, a constant velocity of 6.4 m/s or 16.7 m/s in the Y direction is applied. The initial displacements in the X direction are fixed up to the crack length, as shown by symbol ②. The final

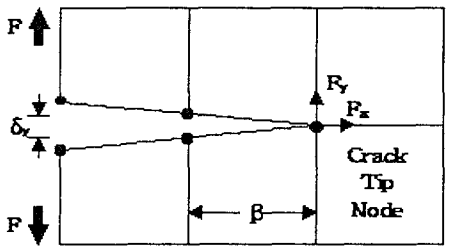

Fig. 5. The nodal force at crack tip.

displacements in X and Y directions are defined as the whole length minus the crack length, as shown by symbol ③. When the crack propagates along the X direction, the displacements in the Y direction on the nodes are released sequentially along the crack line. The crack speeds, crack propagation lengths and time data are taken from the experimental data. The hard contact between end-block and pin is labeled as the symbol ④ and the tied contact is established between block and specimen as shown by the symbol ⑤. In simulation, the mechanical properties of the specimen are the same as the composite used in the experiment, described in section 2.1. The total strain energy release rate, G is obtained by use of the nodal force at crack tip and the displacement of next node on the face of crack mouth as shown in Fig. 5. β is the width of crack tip and F_x, F_y, δ_x and δ_y are the nodal forces and displacements at the respective X and Y directions.

The load (P) applied to this model increases and the critical energy release rate (G_c) at the crack tip was obtained by the formula at this simulation as Eq. (4) [15].

$$G_c=(F_x\delta_x+F_y\delta_y)/(2\beta) \quad (4)$$

3.2 Simulation analysis

Fig. 6 shows the load according to the displacement applied from pin onto end block with experiment and simulation in the case of the test conducted at 6.4 m/s. The load from 400 N to 500 N becomes highest at the displacement of 4 mm at the first time. The load decreases as the displacement increases. The load of 100 N becomes lowest at the range of displacement from 15 mm to 20 mm on the last step. This simulation curve approaches the experimental data.

Fig. 7 shows the energy release rate according to crack length with experiment and simulation in case of the rate of 6.4 m/s. The energy release rate increases to the value of 2920 J/m^2 as the crack length

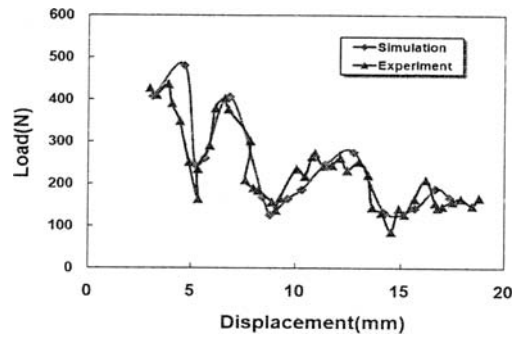

Fig. 6. The load according to the displacement applied from pin onto end block with experiment and simulation in case of the rate of 6.4 m/s.

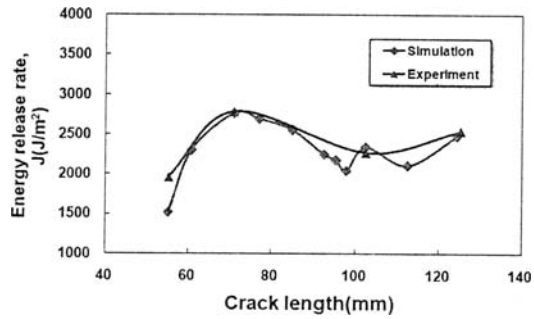

Fig. 7. The energy release rate according to crack length with experiment and simulation in case of the rate of 6.4 m/s.

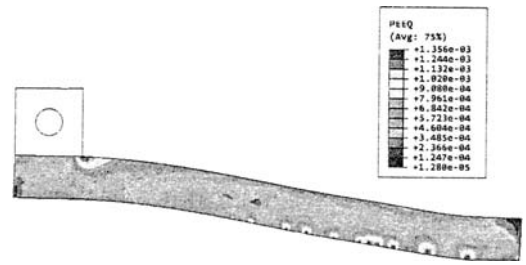

Fig. 8. The contour plot of equivalent plastic strain in specimen in case of the rate of 6.4 m/s (elapsed time of 2.25 × 10^{-4} sec., last step in simulation).

increases until the crack length approaches 70 mm. This energy release rate decreases to the value of 2270 J/m^2 at the range of the crack length from 70 mm to 100 mm followed by the increase up to the value of 2470 J/m^2 at the range of the crack length beyond 100 mm, which agrees well with the experimental data.

Fig. 8 shows simulation results of the rate of 6.4 m/s. The contour lines are the equivalent plastic strains at the time of 22.5 millisecond, which show the equivalent plastic strain of 0.135 % at the crack tip.

In Fig. 9, the load was applied from pin onto end block at the rate of 16.7 m/s. The simulation and experiment compared are in good agreement as shown. The load increases as the displacement increases until the displacement of 7 mm is reached at which the load is a maximum as 350 N. And load, then, turns downwards at around the displacement of 7 mm. The maximum loads from pin onto end block in the increasing impact rates from 6.4 m/s to 16.7 m/s are increased to 500 N (at displacement 7 mm) from 350 N (at displacement 4 mm).

Fig. 10 displays the energy release rate which is corresponding to crack length from the results of experiment and simulation at the rate of 16.7 m/s. In this figure, the energy release rate increases to the value of 2700 J/m^2 as the crack length increases until the crack length of 70 mm beyond which the energy release rate turns to decrease to the value of 2270 J/m^2. As results, the maximum energy releases vary from 2700 J/m^2 to 3000 J/m^2 at the crack length of 70 mm at the impact rates, 6.4 m/s and 16.7 m/s.

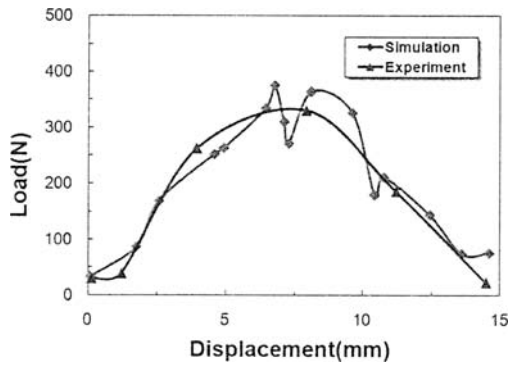

Fig. 9. Displacement vs. load at the rate of 16.7 m/s.

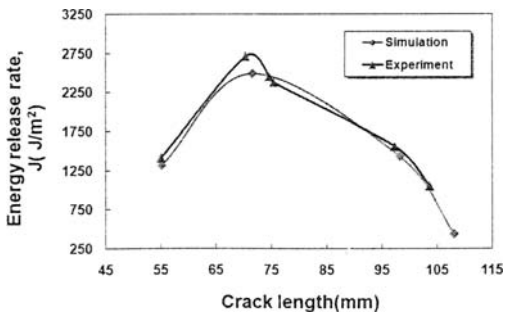

Fig. 10. The energy release rate corresponding to crack length plot at the rate of 16.7 m/s.

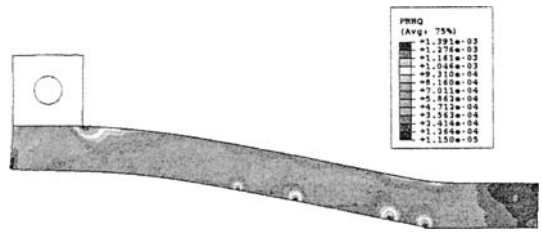

Fig. 11. The contour lines of equivalent plastic strain in specimen at the rate of 16.7 m/s (elapsed time of 1.50 × 10^{-4} sec., last step in simulation).

Fig. 11 shows the contour line plot of equivalent plastic strain in specimen at the time of 15.0 millisecond at the last step in simulation at the rate of 16.7 m/s. Fig. 11 also shows the equivalent plastic strain of 1.39 × 10^{-3} at the crack tip. The values of equivalent plastic strains near the crack tip are within the range from 1.35 × 10^{-3} to 1.39 × 10^{-3} at the impact rates of 6.4 m/s and 16.7 m/s.

4. Conclusion

In this study, the following are deduced from the impact finite element analysis for the nonlinear plastic behavior of the dynamically loaded adhesively-bonded specimens.

A reliable finite element model is proposed and verified to accurately predict impact behavior of a fractured adhesively bonded DCB specimen. Compared to the pre-conducted experiments, the simulated load against the displacement applied from pin onto end block and the energy release rate as a function of crack length in the dynamic experiment were very closely predicted.

Based on the analysis, the values of maximum loads applied from pin onto end block were calculated in the range from 350 N to 500 N in case of the impact rates of 6.4 m/s and 16.7 m/s.

The maximum energy release rates predicted were in the range from 2700 J/ m^2 to 3000 J/ m^2 at the crack length of 70 mm in case of the impact rates of 6.4 m/s and 16.7 m/s.

The values of equivalent plastic strains at the crack tips were within the range from 1.35 × 10^{-3} to 1.39 × 10^{-3} in case of the impact rates of 6.4 m/s and 16.7 m/s.

Acknowledgement

"This work was supported by the Korea Research Foundation Grant." (KRF-2006-013-D00179)

References

[1] I. Norio, Y. Kejian and S. Akenori, Dynamic non-linear analysis of reinforced concrete shear wall by finite element method with explicit analytical procedure, *Earthquake Engineering & Structural Dynamics.* 26(9) (1997) 967-986.

[2] S. B. Biner, A finite element method analysis of the role of interface behavior in the creep rupture characteristics of a discontinuously reinforced composite with sliding grain boundaries, *Materials Science & Engineering. Properties, Microstructure and Processing. A, Structural Materials.* 208(2) (1996) 239-248.

[3] B. R. K. Blackman, J. P. Dear, A. J. Kinloch, H. MacGillivray, Y. Wang, J.G.Williams and P.Yayla, Failure of fiber composites and adhesively bonded fiber composites under high rates of test part III mixed-mode I/II and mode II loadings, *Journal of Materials Science.* 31(17) (1996) 4467-4477.

[4] M. Kawai and Y. Masuko, Creep behavior of unidirectional and angle-ply T800H/3631 laminates at high temperature and simulations using a phenomenological viscoplasticity model, *Composites Science and Technology.* 64(15) (2004) 2373-2384.

[5] X. J. Yang, Constitutive description of temperature-dependent nonproportional cyclic viscoplasticity, *Journal of Engineering Materials and Technology.* 119(1) (1997) 12-19.

[6] A. S. Chen, D. P. Almond and B. Harris, Impact damage growth in composites under fatigue conditions monitored by acoustography, *International Journal of Fatigue.* 24(2/4) (2002) 257-261.

[7] I. Georgiou, A. Ivankovic, A. J. Kinloch and V. Tropsa, Rate dependent fracture behaviour of adhesively bonded joints, *Fracture of Polymers, Composites and Adhesives.* (2003) 317-328.

[8] A. Tabiei, W. Yi and R. Goldberg, Non-linear strain rate dependent micro-mechanical composite material model for finite element impact and crash worthiness simulation, *International Journal of Non-linear Mechanics.* 40(7) (2005) 957-970.

[9] International Standards Organisation, ISO 11343 (ISO, Geneva) (1993).

[10] ABAQUS Manual, Version 6.6, Karlsson and Sorensen Inc. (2006).

[11] B. R. Blackman, J. P. Dear, A. J. Kinloch, H. Macgillivray, The faliure of fiber composites and adhesively bonded fiber composites under high rates of test, *Journal of Materials Science.* 30 (1995) 5885-5900.

[12] B. R. Blackman, A. J. Kinloch and J. G. Williams, The failure of fiber composites and adhesively bonded fiber composites under high rates of test. part 3, *Journal of Material Science.* 31 (1996) 4467-4477.

[13] J. G. Williams, End corrections for orthotropic DCB specimens, *Compos Sci Technol.* 35 (1989) 367-376.

[14] J. G. Williams, Large displacement and end block effects in the DCB interlaminar test in modes I & II, *Journal of Compos Mater.* 21 (1987) 330-347.

[15] E. F. Rybicki and M. F. Kanninen, A finite element calculation of stress intensity factors by a modified crack closure integral, *Engineering Fracture Mechanics.* 9 (4) (1977) 753-976.